

Model Order Reduction for Nonlinear Radiative Transfer Based on Moment Equations and Data-Driven Approximations of the Eddington Tensor

Joseph M. Coale

Department of Nuclear Engineering
North Carolina State University

Los Alamos National Laboratory

- Fundamental approach and basic ideas
 - Model order reduction for Boltzmann transport problems
 - Thermal radiative transfer (TRT) problems
 - Nonlinear projective approach
- Derivation of multilevel low-order Quasidiffusion (Variable Eddington Factor) equations for the Boltzmann transport equation (BTE)
- Formulation of data-driven ROMs for nonlinear TRT problems with POD and DMD of the Eddington tensor
- Numerical results for multigroup TRT problems in 2D Cartesian geometry
- Discussion
- This is a joint work with Dmitriy Anistratov (NCSU)

- Radiative transfer is the physical process of energy transfer via the propagation, emission and absorption of photon radiation in the host medium
- Radiative transfer becomes the dominant mode of energy redistribution in materials at extreme temperatures, and is an essential piece of physics for many phenomena spanning several fields
 - plasma physics
 - high-energy density physics
 - astrophysics
 - atmospheric science
- These phenomena are described by complex multiphysical systems of differential equations (radiation hydrodynamics)
- The particle transport physics is modeled by the Boltzmann transport equation (BTE)

Challenges in Simulation of Particle Transport Problems

- The numerical simulation of multiphysical particle transport problems faces several challenges
 - High-dimensionality
 - Strong nonlinearity
 - Strong coupling of equations
 - Material opacities depend on state of matter
 - The state of matter is influenced by particle fluxes
 - Multi-scale characterization
 - Distinct characteristic behavior in different energy ranges
 - System of equations of different types
 - Integro-differential BTE
- The BTE is especially challenging to solve
 - Hyperbolic differential operator
 - The solution at any point depends on the solution everywhere in phase space due to the integral operator
 - The solution is high-dimensional

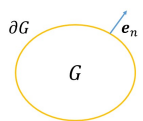
- The BTE largely influences the dimensionality of these problems
 - 3D geometry \rightarrow 7 independent variables
- Reduced order models (ROMs) for the BTE are commonly employed to reduce the cost of multiphysics simulations involving radiative transfer
- Some ROMs have seen widespread adoption for their usefulness and simplicity
 - Diffusion-based models like flux limited diffusion (FLD)
 - P_1 , $P_{1/3}$, P_3
 - Minerbo models
- However, the accuracy of these models is limited
- The development of *advanced* ROMs for the BTE that can achieve both computational efficiency and high accuracy is an active field of research
 - In recent times the bulk of this research effort has been focused on data-driven ROMs

- The most advanced methods for data-driven model order reduction were developed with fluid dynamics in mind
- More recently these methods have been the subject of a substantial research effort for developing ROMs for Boltzmann transport
- The majority of these ROMs focus on linear particle transport problems
- Many questions remain for nonlinear problems of high energy density physics (radiation hydrodynamics problems)
 - How to preserve and reproduce essential features of fundamental physics
 - Dealing with multiscale behavior

- Nonlinear projective approach
 - interpretation
 - nonlinear method of moments
 - multigrid approach
 - Known to give advantage in multiphysical, multiscale applications
- The BTE is coupled with a hierarchy of low-order moment equations
 - Each moment system is exactly closed through nonlinear functionals of the BTE solution (e.g. the Eddington tensor)
 - Moment equations are conservation equations for integral (low-dimensional) quantities
 - Moment equations account for different scales of the problem
 - Multiphysics equations are coupled to moment equations on the same dimensional scale
- Data-driven methods of approximation to estimate closures for low-order equations
 - proper orthogonal decomposition (POD)
 - dynamic mode decomposition (DMD)
 - Fundamental radiation physics conserved through moment equations

Nonlinear Thermal Radiative Transfer Problem

- Prototypes of these ROMs are designed for the fundamental thermal radiative transfer (TRT) problem
 - Supersonic radiation flow problem neglecting material motion, photon scattering, heat conduction and external sources
- The high-order multigroup Boltzmann transport equation (BTE)

$$\frac{1}{c} \frac{\partial I_g(\mathbf{r}, \boldsymbol{\Omega}, t)}{\partial t} + \boldsymbol{\Omega} \cdot \nabla I_g(\mathbf{r}, \boldsymbol{\Omega}, t) + \kappa_g(T) I_g(\mathbf{r}, \boldsymbol{\Omega}, t) = \kappa_g(T) B_g(T)$$


$\mathbf{r} \in G$, for all $\boldsymbol{\Omega}$, $g = 1, \dots, N_g$, $t \geq t_0$,
 $I_g|_{\mathbf{r} \in \partial G} = I_g^{in}$, $\boldsymbol{\Omega} \cdot \mathbf{e}_n < 0$, $t \geq t_0$,
 $I_g|_{t=t_0} = I_g^0$, $\mathbf{r} \in G$, for all $\boldsymbol{\Omega}$,

- \mathbf{r} - spatial position, $\boldsymbol{\Omega}$ - direction of particle motion, g - photon frequency group, t - time, $I_g(\mathbf{r}, \boldsymbol{\Omega}, t)$ - specific intensity of photons in the group g
- The material energy balance (MEB) equation

$$\frac{\partial \varepsilon(T)}{\partial t} = \sum_{g=1}^{N_g} \int_{4\pi} \kappa_g(T) \left(I_g(\mathbf{r}, \boldsymbol{\Omega}, t) - B_g(T) \right) d\boldsymbol{\Omega}, \quad T|_{t=t_0} = T^0(\mathbf{r}), \text{ for } \mathbf{r} \in G.$$

$$\frac{1}{c} \frac{\partial I_g}{\partial t} + \Omega \cdot \nabla I_g + \kappa_g(T) I_g = \kappa_g(T) B_g(T)$$

- Angular moments of intensities

- $$E_g(r, t) = \frac{1}{c} \int_{4\pi} I_g d\Omega$$

- $$\mathbf{F}_g(r, t) = \int_{4\pi} \Omega I_g d\Omega$$

- Projection: $\int_{4\pi} \cdot d\Omega$ $\int_{4\pi} \Omega \cdot d\Omega$

$$\frac{\partial E_g}{\partial t} + \nabla \cdot \mathbf{F}_g + c \kappa_g(T) E_g = 4\pi \kappa_g(T) B_g(T), \quad (1)$$

$$\frac{1}{c} \frac{\partial \mathbf{F}_g}{\partial t} + c \nabla \cdot (\mathbf{f}_g[l] E_g) + \kappa_g(T) \mathbf{F}_g = 0 \quad (2)$$

- Exact closure through the Eddington tensor

$$\mathbf{f}_g[l] = \frac{\int_{4\pi} \Omega \otimes \Omega I_g d\Omega}{\int_{4\pi} I_g d\Omega} \quad (3)$$

$$\frac{1}{c} \frac{\partial I_g}{\partial t} + \Omega \cdot \nabla I_g + \kappa_g(T) I_g = \kappa_g(T) B_g(T)$$

- Angular moments of intensities

- $$E_g(r, t) = \frac{1}{c} \int_{4\pi} I_g d\Omega$$

- $$\mathbf{F}_g(r, t) = \int_{4\pi} \Omega I_g d\Omega$$

- Projection: $\int_{4\pi} \cdot d\Omega$ $\int_{4\pi} \Omega \cdot d\Omega$

$$\frac{\partial E_g}{\partial t} + \nabla \cdot \mathbf{F}_g + c \kappa_g(T) E_g = 4\pi \kappa_g(T) B_g(T), \quad (1)$$

$$\frac{1}{c} \frac{\partial \mathbf{F}_g}{\partial t} + c \nabla \cdot (\mathbf{f}_g[l] E_g) + \kappa_g(T) \mathbf{F}_g = 0 \quad (2)$$

- Exact closure through the Eddington tensor

$$\mathbf{f}_g[l] = \frac{\int_{4\pi} \Omega \otimes \Omega I_g d\Omega}{\int_{4\pi} I_g d\Omega} \quad (3)$$

$$\frac{1}{c} \frac{\partial I_g}{\partial t} + \Omega \cdot \nabla I_g + \kappa_g(T) I_g = \kappa_g(T) B_g(T)$$

- Angular moments of intensities

- $E_g(r, t) = \frac{1}{c} \int_{4\pi} I_g d\Omega$

- $F_g(r, t) = \int_{4\pi} \Omega I_g d\Omega$

- Projection: $\int_{4\pi} \cdot d\Omega$ $\int_{4\pi} \Omega \cdot d\Omega$

$$\frac{\partial E_g}{\partial t} + \nabla \cdot F_g + c \kappa_g(T) E_g = 4\pi \kappa_g(T) B_g(T), \quad (1)$$

$$\frac{1}{c} \frac{\partial F_g}{\partial t} + c \nabla \cdot (\mathbf{f}_g[l] E_g) + \kappa_g(T) F_g = 0 \quad (2)$$

- Exact closure through the Eddington tensor

$$\mathbf{f}_g[l] = \frac{\int_{4\pi} \Omega \otimes \Omega I_g d\Omega}{\int_{4\pi} I_g d\Omega} \quad (3)$$

Effective Grey Quasidiffusion (VEF) Equations

$$\frac{\partial \mathbf{E}_g}{\partial t} + \nabla \cdot \mathbf{F}_g + c \kappa_g(T) E_g = 4\pi \kappa_g(T) B_g(T),$$

$$\frac{1}{c} \frac{\partial \mathbf{F}_g}{\partial t} + c \nabla \cdot (\mathbf{f}_g [I] E_g) + \kappa_g(T) \mathbf{F}_g = 0$$

- Frequency-integrated angular moments of intensities

- $E = \sum_{g=1}^{N_g} E_g, \quad \mathbf{F} = \sum_{g=1}^{N_g} \mathbf{F}_g$

- Projection: $\sum_{g=1}^{N_g} \cdot$

$$\frac{\partial E}{\partial t} + \nabla \cdot \mathbf{F} + c \bar{\kappa}_E E = c \bar{\kappa}_{B,R} T^4 \quad (4)$$

$$\frac{1}{c} \frac{\partial \mathbf{F}}{\partial t} + c \nabla \cdot (\bar{\mathbf{f}} E) + \bar{\mathbf{K}}_R \mathbf{F} + \bar{\eta} E = 0 \quad (5)$$

- Exact closure through frequency-averaged grey factors

$$\bar{\kappa}_E = \frac{\sum_{g=1}^{N_g} \kappa_g E_g}{\sum_{g=1}^{N_g} E_g}, \quad \bar{\kappa}_B = \frac{\sum_{g=1}^{N_g} \kappa_g B_g}{\sum_{g=1}^{N_g} B_g}, \quad \bar{\kappa}_{R,\alpha} = \frac{\sum_{g=1}^{N_g} \kappa_g |F_{\alpha,g}|}{\sum_{g=1}^{N_g} |F_{\alpha,g}|}, \quad (6)$$

$$\mathbf{K}_R = \text{diag}(\bar{\kappa}_{R,x}, \bar{\kappa}_{R,y}, \bar{\kappa}_{R,z}), \quad \bar{\mathbf{f}} = \frac{\sum_{g=1}^{N_g} \mathbf{f}_g E_g}{\sum_{g=1}^{N_g} E_g}, \quad \bar{\eta} = \frac{\sum_{g=1}^{N_g} (\kappa_g - \bar{\mathbf{K}}_R) \mathbf{F}_g}{\sum_{g=1}^{N_g} E_g}. \quad (7)$$

Effective Grey Quasidiffusion (VEF) Equations

$$\frac{\partial \mathbf{E}_g}{\partial t} + \nabla \cdot \mathbf{F}_g + c\kappa_g(T)E_g = 4\pi\kappa_g(T)B_g(T),$$

$$\frac{1}{c} \frac{\partial \mathbf{F}_g}{\partial t} + c\nabla \cdot (\mathbf{f}_g[I]E_g) + \kappa_g(T)\mathbf{F}_g = 0$$

- Frequency-integrated angular moments of intensities

- $E = \sum_{g=1}^{N_g} E_g, \quad \mathbf{F} = \sum_{g=1}^{N_g} \mathbf{F}_g$

- Projection: $\sum_{g=1}^{N_g} \cdot$

$$\frac{\partial E}{\partial t} + \nabla \cdot \mathbf{F} + c\bar{\kappa}_E E = c\bar{\kappa}_B a_R T^4 \quad (4)$$

$$\frac{1}{c} \frac{\partial \mathbf{F}}{\partial t} + c\nabla \cdot (\bar{\mathbf{f}}E) + \bar{\mathbf{K}}_R \mathbf{F} + \bar{\eta}E = 0 \quad (5)$$

- Exact closure through frequency-averaged grey factors

$$\bar{\kappa}_E = \frac{\sum_{g=1}^{N_g} \kappa_g E_g}{\sum_{g=1}^{N_g} E_g}, \quad \bar{\kappa}_B = \frac{\sum_{g=1}^{N_g} \kappa_g B_g}{\sum_{g=1}^{N_g} B_g}, \quad \bar{\kappa}_{R,\alpha} = \frac{\sum_{g=1}^{N_g} \kappa_g |F_{\alpha,g}|}{\sum_{g=1}^{N_g} |F_{\alpha,g}|}, \quad (6)$$

$$\mathbf{K}_R = \text{diag}(\bar{\kappa}_{R,x}, \bar{\kappa}_{R,y}, \bar{\kappa}_{R,z}), \quad \bar{\mathbf{f}} = \frac{\sum_{g=1}^{N_g} \mathbf{f}_g E_g}{\sum_{g=1}^{N_g} E_g}, \quad \bar{\eta} = \frac{\sum_{g=1}^{N_g} (\kappa_g - \bar{\mathbf{K}}_R) \mathbf{F}_g}{\sum_{g=1}^{N_g} E_g}. \quad (7)$$

Multilevel Quasidiffusion Method

- High-order Boltzmann transport equation for I_g

$$\frac{1}{c} \frac{\partial I_g}{\partial t} + \Omega \cdot \nabla I_g + \kappa_g(T) I_g = \kappa_g(T) B_g(T)$$

- Eddington tensor $I_g \Rightarrow \mathbf{f}_g[I] = \frac{\int_{4\pi} \Omega \otimes \Omega I_g d\Omega}{\int_{4\pi} I_g d\Omega}$

- Multigroup quasidiffusion equations for E_g , F_g

$$\frac{\partial E_g}{\partial t} + \nabla \cdot \mathbf{F}_g + c \kappa_g(T) E_g = 4\pi \kappa_g(T) B_g(T),$$

$$\frac{1}{c} \frac{\partial \mathbf{F}_g}{\partial t} + c \nabla \cdot (\mathbf{f}_g[I] E_g) + \kappa_g(T) \mathbf{F}_g = 0$$

- Grey closures E_g , $F_g \Rightarrow \bar{\chi}_E, \bar{\chi}_B, \bar{\mathbf{f}}, \bar{K}_R, \bar{\eta}$

- Effective grey problem for E , F , T

$$\frac{\partial E}{\partial t} + \nabla \cdot \mathbf{F} + c \bar{\chi}_E E = c \bar{\chi}_B a_R T^4$$

$$\frac{1}{c} \frac{\partial \mathbf{F}}{\partial t} + c \nabla \cdot (\bar{\mathbf{f}} E) + \bar{K}_R \mathbf{F} + \bar{\eta} E = 0$$

$$\frac{\partial \varepsilon(T)}{\partial t} = c (\bar{\chi}_E E - \bar{\chi}_B a_R T^4)$$

$$\bar{\chi}_E = \frac{\sum_{g=1}^{N_g} \kappa_g E_g}{\sum_{g=1}^{N_g} E_g}$$

$$\bar{\chi}_B = \frac{\sum_{g=1}^{N_g} \kappa_g B_g}{\sum_{g=1}^{N_g} B_g}$$

$$\bar{\chi}_{R,\alpha} = \frac{\sum_{g=1}^{N_g} \kappa_g |F_{\alpha,g}|}{\sum_{g=1}^{N_g} |F_{\alpha,g}|}$$

$$\mathbf{K}_R = \text{diag}(\bar{\chi}_{R,x}, \bar{\chi}_{R,y}, \bar{\chi}_{R,z})$$

$$\bar{\mathbf{f}} = \frac{\sum_{g=1}^{N_g} \mathbf{f}_g E_g}{\sum_{g=1}^{N_g} E_g}$$

$$\bar{\eta} = \frac{\sum_{g=1}^{N_g} (\kappa_g - \bar{K}_R) F_g}{\sum_{g=1}^{N_g} E_g}$$

Reduced-Order Model for TRT

- Data-driven approximator

$$\tilde{\mathbf{f}}_g = \mathcal{G}[\mathbf{f}^*], \quad \mathbf{f}^* \text{ known}$$

- Multigroup quasidiffusion equations for E_g , \mathbf{F}_g

$$\frac{\partial E_g}{\partial t} + \nabla \cdot \mathbf{F}_g + c \kappa_g(T) E_g = 4\pi \kappa_g(T) B_g(T),$$

$$\frac{1}{c} \frac{\partial \mathbf{F}_g}{\partial t} + c \nabla \cdot (\tilde{\mathbf{f}}_g E_g) + \kappa_g(T) \mathbf{F}_g = 0$$

- Grey closures E_g , $\mathbf{F}_g \Rightarrow \bar{\chi}_E, \bar{\chi}_B, \bar{\mathbf{f}}, \bar{\mathbf{K}}_R, \bar{\eta}$

- Effective grey problem for E , \mathbf{F} , T

$$\frac{\partial E}{\partial t} + \nabla \cdot \mathbf{F} + c \bar{\chi}_E E = c \bar{\chi}_B a_R T^4$$

$$\frac{1}{c} \frac{\partial \mathbf{F}}{\partial t} + c \nabla \cdot (\bar{\mathbf{f}} E) + \bar{\mathbf{K}}_R \mathbf{F} + \bar{\eta} E = 0$$

$$\frac{\partial \varepsilon(T)}{\partial t} = c (\bar{\chi}_E E - \bar{\chi}_B a_R T^4)$$

$$\bar{\chi}_E = \frac{\sum_{g=1}^{N_g} \kappa_g E_g}{\sum_{g=1}^{N_g} E_g}$$

$$\bar{\chi}_B = \frac{\sum_{g=1}^{N_g} \kappa_g B_g}{\sum_{g=1}^{N_g} B_g}$$

$$\bar{\chi}_{R,\alpha} = \frac{\sum_{g=1}^{N_g} \kappa_g |F_{\alpha,g}|}{\sum_{g=1}^{N_g} |F_{\alpha,g}|}$$

$$\bar{\mathbf{K}}_R = \text{diag}(\bar{\chi}_{R,x}, \bar{\chi}_{R,y}, \bar{\chi}_{R,z})$$

$$\bar{\mathbf{f}} = \frac{\sum_{g=1}^{N_g} \mathbf{f}_g E_g}{\sum_{g=1}^{N_g} E_g}$$

$$\bar{\eta} = \frac{\sum_{g=1}^{N_g} (\kappa_g - \bar{\mathbf{K}}_R) \mathbf{F}_g}{\sum_{g=1}^{N_g} E_g}$$

- Projection, compression of data
 - Given: full-order solution to some TRT problem for N_t time steps, N_g frequency groups, N_r spatial cells
 - Vectors of each Eddington Tensor component at time t^n

$$\mathbf{f}_{\alpha\beta}^n \in \mathbb{R}^{N_r N_g}, \quad \alpha, \beta = x, y, z$$

- Construction of snapshot matrices

$$\mathbf{A}^{\mathbf{f}_{\alpha\beta}} = [\mathbf{f}_{\alpha\beta}^1 \ \mathbf{f}_{\alpha\beta}^2 \ \dots \ \mathbf{f}_{\alpha\beta}^{N_t}] \in \mathbb{R}^{N_r N_g \times N_t}$$

- Define projection operator \mathcal{G}^k that will project a given matrix \mathbf{A} onto a rank- k subspace

$$\mathcal{A}_k^{\mathbf{f}_{\alpha\beta}} = \mathcal{G}^k \mathbf{A}^{\mathbf{f}_{\alpha\beta}}, \quad k \leq \text{rank}(\mathbf{A}^{\mathbf{f}_{\alpha\beta}})$$

- $\mathcal{A}_k^{\mathbf{f}_{\alpha\beta}}$ is constructed of k sets of various vectors and factors
- Approximation of data from rank k representation
 - A map \mathcal{M}^n is defined by the same method used to define \mathcal{G}^k

$$\mathbf{f}_{\alpha\beta}^n \approx \mathcal{M}^n \mathcal{A}_k^{\mathbf{f}_{\alpha\beta}}$$

POD of the Eddington Tensor

- Centered data matrix

$$\hat{\mathbf{A}}^{\mathbf{f}_{\alpha\beta}} = [\hat{\mathbf{f}}_{\alpha\beta}^1, \dots, \hat{\mathbf{f}}_{\alpha\beta}^{N_t}], \quad \hat{\mathbf{f}}_{\alpha\beta}^n = \mathbf{f}_{\alpha\beta}^n - \bar{\mathbf{f}}_{\alpha\beta}, \quad \bar{\mathbf{f}}_{\alpha\beta} = \frac{1}{N_t} \sum_{n=1}^{N_t} \mathbf{f}_{\alpha\beta}^n$$

- A thin singular value decomposition (SVD) represents the matrix in the form

$$\hat{\mathbf{A}}^{\mathbf{f}_{\alpha\beta}} = \mathbf{U}\mathbf{S}\mathbf{V}^T,$$

$\mathbf{U} \in \mathbb{R}^{N_r N_g, d}$ holds the left singular vectors $\{\mathbf{u}_\ell\}_{\ell=1}^d$ in its columns

$\mathbf{V} \in \mathbb{R}^{N_t, d}$ holds the right singular vectors $\{\mathbf{v}_\ell\}_{\ell=1}^d$ in its columns

$\mathbf{S} \in \mathbb{R}^{d, d}$ holds the singular values $\{\sigma_\ell\}_{\ell=1}^d$ along its diagonal in decreasing order,

$$d = \text{rank}(\hat{\mathbf{A}}^{\mathbf{f}_{\alpha\beta}}) = \min(N_r N_g, N_t)$$

- The rank- k POD representation of $\mathbf{f}_{\alpha\beta}$

$$\mathcal{A}_k^{\mathbf{f}_{\alpha\beta}} = \bar{\mathbf{f}}_{\alpha\beta} \cup \{\sigma_\ell, \mathbf{u}_\ell, \mathbf{v}_\ell\}_{\ell=1}^k$$

$$\tilde{\mathbf{f}}_{\alpha\beta}^n \leftarrow \bar{\mathbf{f}}_{\alpha\beta} + \sum_{\ell=1}^k \sigma_\ell (\mathbf{v}_\ell)_n \mathbf{u}_\ell = \mathcal{M}^n \mathcal{A}_k^{\mathbf{f}_{\alpha\beta}}$$

DMD of the Eddington Tensor

- The DMD constructs the best-fit linear operator \mathbf{B} to the time-dependent data $\{\mathbf{f}_{\alpha\beta}^n\}_{n=1}^{N_t}$, generating the dynamic system:

$$\frac{d\tilde{\mathbf{f}}_{\alpha\beta}(t)}{dt} = \mathbf{B}\tilde{\mathbf{f}}_{\alpha\beta}(t), \quad \Rightarrow \quad \tilde{\mathbf{f}}_{\alpha\beta}(t) = \sum_{\ell=1}^k \beta_{\ell} \varphi_{\ell} e^{\omega_{\ell} t},$$

$\omega_{\ell}, \varphi_{\ell}$ are the eigenvalues and associated eigenfunctions of \mathbf{B}

- Form two data matrices for $t^n = t^{n-1} + \Delta t$ with constant time step

$$\mathbf{X}_{\alpha\beta} = [\mathbf{f}_{\alpha\beta}^1, \dots, \mathbf{f}_{\alpha\beta}^{N_t-1}], \quad \hat{\mathbf{X}}_{\alpha\beta} = [\mathbf{f}_{\alpha\beta}^2, \dots, \mathbf{f}_{\alpha\beta}^{N_t}] \quad \mathbf{f}_{\alpha\beta}^n \in \mathbb{R}^{N_r N_g}$$

- $\tilde{\mathbf{B}} = \hat{\mathbf{X}}\mathbf{X}^+$ is the closest approximation to \mathbf{B} in the Frobenius norm. Here $+$ signifies the Moore-Penrose pseudo inverse.
- The DMD representation

$$\mathcal{A}_k^{\mathbf{f}_{\alpha\beta}} = \{\tilde{\beta}_{\ell}, \tilde{\omega}_{\ell}, \tilde{\varphi}_{\ell}\}_{\ell=1}^k, \quad \tilde{\mathbf{f}}_{\alpha\beta}(t^n) = \sum_{\ell=1}^k \tilde{\beta}_{\ell} \tilde{\varphi}_{\ell} e^{\tilde{\omega}_{\ell} t^n}, \quad \tilde{\omega}_{\ell} = \Delta t^{-1} \ln(\gamma_{\ell}),$$

where $\gamma_{\ell}, \tilde{\varphi}_{\ell}$ are the eigenvalues and associated eigenfunctions of $\tilde{\mathbf{B}}$

- Equilibrium-subtracted DMD (DMD-E)
 - Construction of the linear operator \mathbf{B} that fits the equilibrium-subtracted data
 - The time-dependent TRT problem tends to steady-state as $t \rightarrow \infty$.

- For each data matrix \mathbf{A} , the rank k must be calculated to store \mathcal{A}_k
- We consider the rank- k truncated SVD

$$\mathbf{A} \approx \mathbf{A}_k = \mathbf{U}_k \mathbf{S}_k \mathbf{V}_k^T$$
$$\mathbf{U}_k = [\mathbf{u}_1 \dots \mathbf{u}_k], \quad \mathbf{S}_k = \text{diag}(\sigma_1, \dots, \sigma_k), \quad \mathbf{V}_k = [\mathbf{v}_1 \dots \mathbf{v}_k]$$

- The error in Frobenius norm

$$\|\mathbf{A} - \mathbf{A}_k\|_F^2 = \sum_{\ell=k+1}^d \sigma_\ell^2$$

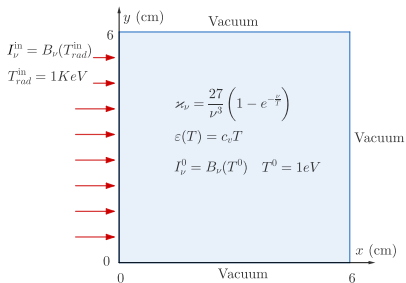
- We calculate k by choosing the relative Frobenius norm error ξ_{rel}

$$\xi_{\text{rel}}^2 = \frac{\sum_{\ell=k+1}^d \sigma_\ell^2}{\sum_{\ell=1}^d \sigma_\ell^2} = \frac{\|\mathbf{A} - \mathbf{A}_k\|_F^2}{\|\mathbf{A}\|_F^2}$$

- k increases as ξ_{rel} decreases
 - Increasing k increases cost in calculating approximate closures
 - Accuracy is also expected to increase with k

- We do not have theory to predict how the models will perform
- Numerical testing is used to demonstrate the following
 - The models converge to the reference solution as $k \rightarrow d$
 - How the ROM errors converge as $k \rightarrow d$
 - How well the *low-rank* ROMs capture fundamental physics in the solution compared to the full-order TRT model on a given phase-space and time

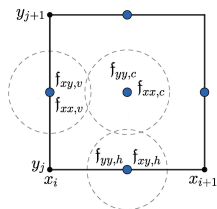
Numerical Test Problem



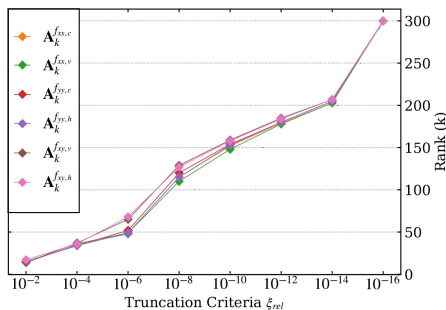
- We test this method on a 2D extension of the Fleck-Cummings (F-C) test
- Fully-implicit time integration
- BTE discretized with simple corner balance scheme
- All low-order equations discretized with 2nd order finite volumes
- Grid:
 - 20x20 spatial cells, 17 groups, 144 discrete directions
 - 300 time steps $\Delta t = .02\text{ns}$ for $0 \leq t \leq 6\text{ns}$
- Degrees of freedom: 1.175×10^9
- ROM degrees of freedom: 1.728×10^7

Numerical Results (POD)

- Databases are formed from the full-order model solution
- Ranks of approximation and memory requirements for the POD with varying ξ_{rel}



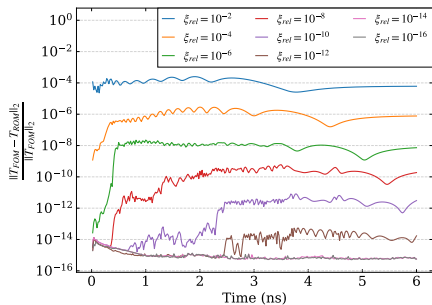
- $I : N_x N_y N_\Omega N_g \times N_t = 1.18 \times 10^9$
- $\mathbf{A}^{f_{xx,c}} : N_x N_y N_g \times N_t = 2.04 \times 10^6$
- $\mathcal{A}_k^{f_{xx,c}} : k(1 + N_t) + (k + 1)N_x N_y N_g$
- $\xi_{rel} = 10^{-2} \rightarrow k = 15 : 1.13 \times 10^5$
- $\xi_{rel} = 10^{-4} \rightarrow k = 34 : 2.48 \times 10^5$



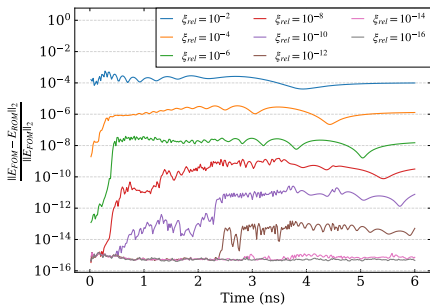
Ranks k vs parameter ξ_{rel}

Numerical Results (POD)

- Relative errors in the 2-norm using the POD compared to the full-order solution
- Errors plotted vs time, each curve corresponds to a value for ξ_{rel}



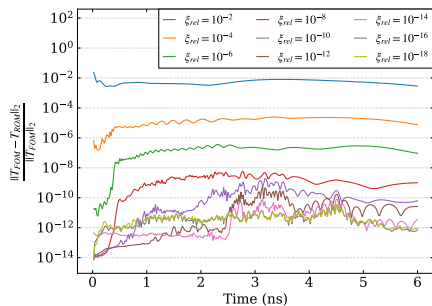
Material Temperature



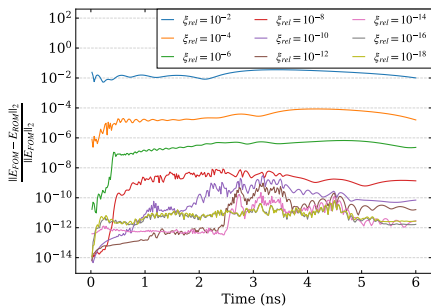
Radiation Energy Density

Numerical Results (DMD)

- Relative errors in the 2-norm using the DMD compared to the full-order solution
- Errors plotted vs time, each curve corresponds to a value for ξ_{rel}



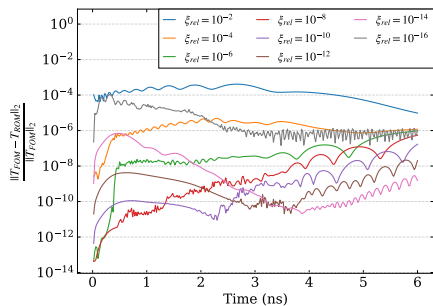
Material Temperature



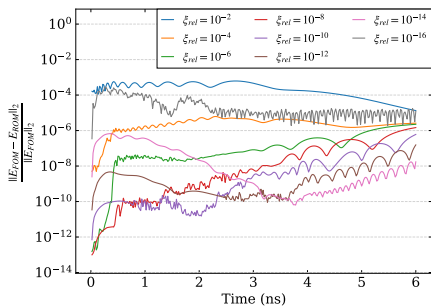
Radiation Energy Density

Numerical Results (DMD-E)

- Relative errors in the 2-norm using the DMD-E compared to the full-order solution
- Errors plotted vs time, each curve corresponds to a value for ξ_{rel}



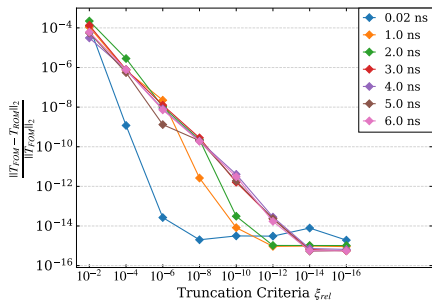
Material Temperature



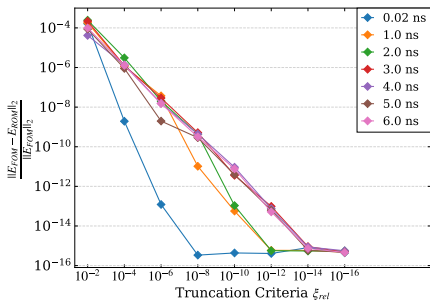
Radiation Energy Density

Convergence of the ROM with Rank (POD)

- Relative errors in the 2-norm using the POD compared to the full-order solution
- Errors plotted vs ξ_{rel} , each curve corresponds to an instant of time



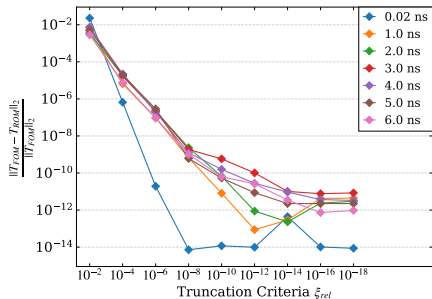
Material Temperature



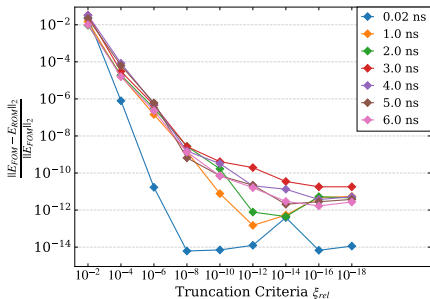
Radiation Energy Density

Convergence of the ROM with Rank (DMD)

- Relative errors in the 2-norm using the DMD compared to the full-order solution
- Errors plotted vs ξ_{rel} , each curve corresponds to an instant of time



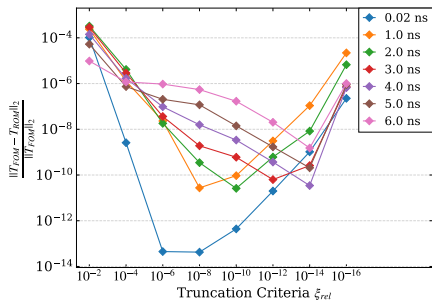
Material Temperature



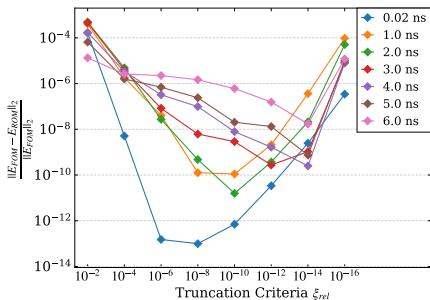
Radiation Energy Density

Convergence of the ROM with Rank (DMD-E)

- Relative errors in the 2-norm using the DMD-E compared to the full-order solution
- Errors plotted vs ξ_{rel} , each curve corresponds to an instant of time



Material Temperature



Radiation Energy Density

- To demonstrate how the low-rank ROMs conserve fundamental physics in the TRT solution, we consider breakout time
- Breakout time is an important measurement in high-temperature laser-driven radiation shock experiments
- For the F-C test we can calculate how well the ROMs capture certain quantities on the right boundary as time elapses
- Total radiation energy density (\bar{E}_R) and material temperature (\bar{T}_R) averaged over the right boundary of the spatial domain vs time

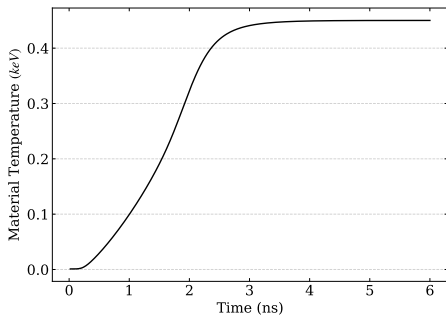
$$\bar{T}_R = \frac{1}{L_R} \int_0^{L_R} T(x_R, y) dy, \quad \bar{E}_R = \frac{1}{L_R} \int_0^{L_R} E(x_R, y) dy$$

- We also consider the spectrum of radiation present at the right boundary

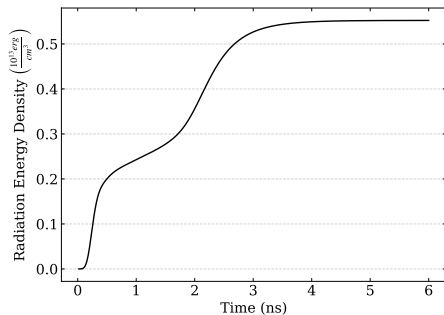
$$\bar{E}_{R,g} = \frac{1}{L_R} \int_0^{L_R} E_g(x_R, y) dy$$

- Total radiation energy density (\bar{E}_R) and material temperature (\bar{T}_R) averaged over the right boundary of the spatial domain vs time

$$\bar{T}_R = \frac{1}{L_R} \int_0^{L_R} T(x_R, y) dy, \quad \bar{E}_R = \frac{1}{L_R} \int_0^{L_R} E(x_R, y) dy$$



\bar{T}_R

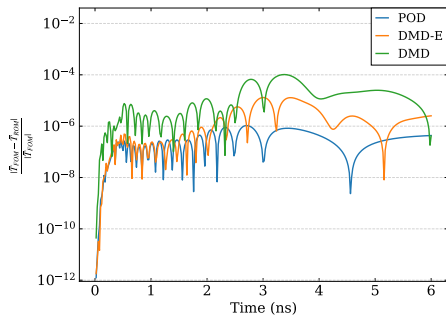


\bar{E}_R

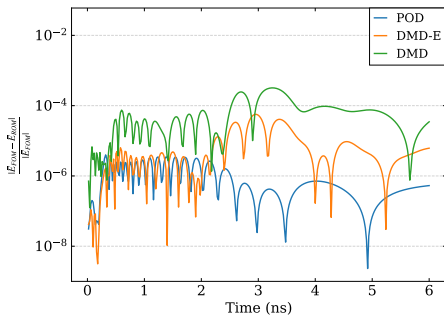
Breakout Time: Relative Error for the ROMs

- $\xi_{\text{rel}} = 10^{-4}$

$$\bar{T}_R = \frac{1}{L_R} \int_0^{L_R} T(x_R, y) dy, \quad \bar{E}_R = \frac{1}{L_R} \int_0^{L_R} E(x_R, y) dy$$

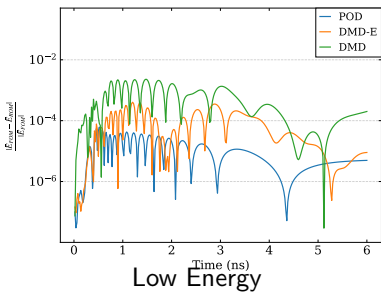


\bar{T}_R



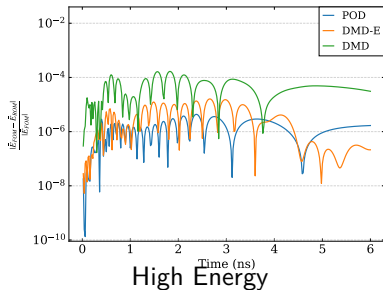
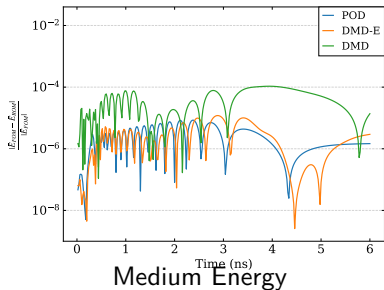
\bar{E}_R

Breakout Time: Relative Error for the DDET ROMs



• $\xi_{rel} = 10^{-4}$

$$\bar{E}_{R,g} = \frac{1}{L_R} \int_0^{L_R} E_g(x_R, y) dy$$



- Main elements of the developed methodology
 - nonlinear projection of the BTE and formulation of a hierarchy of low-order moment equations
 - data-driven techniques to approximate closures
- All models require data on the BTE solution
- The proposed methods have been shown to perform well on highly nonlinear thermal radiative transfer problems
- Any multiphysical equations of interest can be coupled with the effective grey QD equations
- Use of the low-order moment equations enforces conservation of fundamental physics in radiative transfer component
- The proposed approach for development of ROMs can be applied to a wide class of multiphysical high-energy density problems, such as radiative hydrodynamics problems.
- Future research items
 - Optimal sampling techniques for generation of data to inform and train ROMs for TRT
 - Investigation of more complex data-driven methods for approximation
 - Parametrized ROMs for TRT

- J. Coale and D. Anistratov, A reduced-order model for thermal radiative transfer problems based on multilevel quasidiffusion method, *Proc. of Int. Conf. on Mathematics and Computational Methods Applied to Nuclear Science and Engineering M&C 2019*, Portland, OR.
- J. Coale and D. Anistratov, Data-driven grey reduced-order model for thermal radiative transfer problems based on low-order quasidiffusion equations and proper orthogonal decomposition, *Transactions of American Nuclear Society*, **121** (2019)
- J. Coale and D. Anistratov, Reduced order models for nonlinear radiative transfer based on moment equations and POD/DMD of Eddington tensor, *arXiv*: 2107.09174 (2021)
- J. Coale and D. Anistratov, Reduced-order models for thermal radiative transfer based on POD-Galerkin method and low-order quasidiffusion equations, *Proc. of Int. Conf. on Mathematics and Computational Methods Applied to Nuclear Science and Engineering M&C 2021*, Raleigh, NC.

Questions?